Vehicle Description Form

Human Powered Vehicle Challenge 2013

(Form 6)

Latin America: Univ Simon Bolivar, Caracas, Venezuela Feb 22-24
West: NASA Ames Research Ctr, Moffett Field, CA April 12-14
East: Ferris State University, Big Rapids, MI April 26-28

http://go.asme.org/HPVC

This required document for all teams is to be incorporated in to your Design Report. Please Observe Your Due Dates **Latin America Feb 1** **WEST March 11** **EAST March 25**

Vehicle Description

Competition Location: West – NASA Ames Research Center
School name: University of Oklahoma
Vehicle name: The Crimson Edge
Vehicle number 74

Vehicle type Unrestricted X Speed _____

Vehicle configuration

Upright _____ Semi-recumbent X
Prone _____ Other (specify) _____

Frame material 4130 Steel
Fairing material(s) Carbon fiber, Nomex honeycomb
Number of wheels 2
Vehicle Dimensions *(please use inches, pounds)*

Length 108 in. Width 36 in.
Height 59 in. Wheelbase 42 in.
Weight Distribution Front unknown* Rear unknown* Total 80 lb (projected)*
Wheel Size Front 20 in. Rear 27.5 in.
Frontal area 1,494 in^2
Steering Front X Rear _____
Braking Front _____ Rear X Both _____
Estimated Cd 65 rev/min

Vehicle history (e.g., has it competed before? where? when?) This vehicle was fabricated this year and has not been in competition before.

*At this time, the vehicle is not able to be weighed for a total weight.

The University of Oklahoma

2013 ASME HPVC – West: NASA Ames Research Center

Unrestricted Class Entry – **Vehicle 74**

Presents

The Crimson Edge

Vehicle Design Report

Team Officers

James Stevens	Team Captain (jstevens@ou.edu)
Jimmy Walta	Design Captain (jimmywalta@ou.edu)
Jordan Whetsell	Fairing Lead (jordan.a.whetsell@ou.edu)
Kaleb Parks	Steering Lead (kparks2009@ou.edu)
Martha Gattenby	Drivetrain Lead (mgattenby@ou.edu)
Paul Cagle	Stabilization Lead (pcagle86@ou.edu)
Dr. Mrinal Saha	Faculty Advisor (msaha@ou.edu)

Team Roster

1. Berit Pearcy
2. Drew Miller
3. Edward Johnson
4. Eric Pyle
5. Ethan Van Meter
6. James Stevens (Team Captain)
7. Jimmy Walta (Design Captain)
8. Jordan Whetsell (Fairing Lead)
9. Kaleb Parks (Steering Lead)
10. Kyle Williams
11. Martha Gattenby (Drivetrain Lead)
12. Paul Cagle (Stabilization Lead)
13. Shashank Ramarao

3-View Drawing of The Crimson Edge

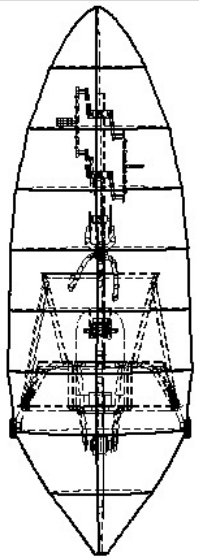

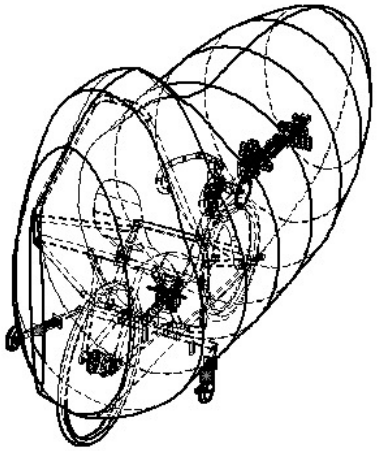

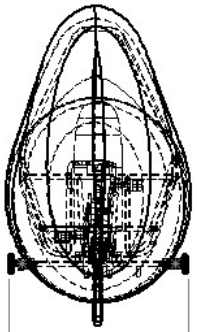

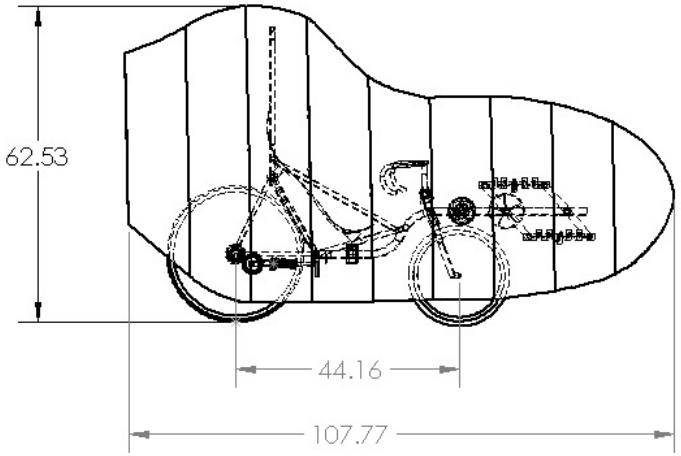

All measurements are in inches.

3/11/13	The Crimson Edge
University of Oklahoma	
ASME HPV Competition - West	

Abstract

The Sooner Powered Vehicle (SPV) team of the University of Oklahoma has designed, built, and tested a competitive recumbent bicycle to participate in the unrestricted class of the American Society of Mechanical Engineers 2013 Human Powered Vehicle Challenge (HPVC) at the NASA Ames facility in California. This year we have introduced three key features in our newly designed vehicle: (i) an adjustable pedaling system, (ii) landing gear support, and (iii) full composite fairing with honeycomb stiffeners. Analyses of both structural and aerodynamic loading were performed to ensure rider protection from rollover and side loadings and to minimize aerodynamic drag force. We used 4130 steel for the frame structure and carbon fiber composite reinforced with honeycomb stiffeners in the fairing to maximize vehicle performance and rider safety. We used light weight foam material to develop the male mold for the composite fairing. The mold surface was coated with fiber glass resin several times, followed by sanding to prepare the mold for layup. Three layers of carbon fiber with epoxy resin were used while applying hand lay-up and vacuum techniques. Several composite panels were fabricated before actual molding took place for process and performance verification. Prototypes for the landing gear support and adjustable pedaling system were also developed for verification of capability and functionality of the components. Finally, combinations of experimental and analytical tools were used to design a safe, practical and high-performance bicycle that should appeal to everyone in the race community.

Table of Contents

Design

a. Objectives

The mission of the University of Oklahoma Sooner Powered Vehicle Team (SPV) is to design, fabricate, and race a competitive recumbent bicycle in order to provide engineering students with the opportunity to demonstrate the application of sound engineering design principles in the development of sustainable and practical transportation alternatives.

This year SPV prepared for an entirely new challenge and design opportunity. In years past, SPV has built and competed with a recumbent trike (3 wheels). However, this year the team decided to design from scratch a new recumbent bicycle (2 wheels) model to be more competitive at the national collegiate level, specifically the American Society of Mechanical Engineers Human Powered Vehicle Challenge competition. Goals for the 2013 vehicle included the following:

- **Safe** for riders, bystanders, and the design team
- **Comfortable** for riders of various sizes
- **Innovative** by bringing new design features to recumbent cycling
- **Stable** for riders of various ability levels
- **Durable** to withstand both competition and utility use

b. Background

The goal of the 2013 SPV team is to raise our level of performance in the ASME HPVC competition in comparison to not only other competing universities, but also to our own university's performance in past years. In order to do this and to outline the basic design goals for this year's vehicle, our team did a thorough analysis of other recumbent bikes to assess what worked, what didn't work, and what we wanted to strive for.

The design element that was first brought forward for consideration was the wheel configuration of the vehicle: a three wheel trike versus a two wheel bike. It was clearly evident from past HPVC results that 2 wheeled vehicles tend to be more competitive, and because our SPV team hasn't built a two wheeled bicycle in the past 5 years, we were ready for a new challenge. To prepare ourselves for an entirely new design concept, our team took a field day to travel to Oklahoma Recumbent Road Bikes, a recumbent bicycle shop in Lexington, Oklahoma, to test two wheeled recumbents for ourselves and to gather ideas from which to base our designs. Additional design aspects that were assessed were drivetrain designs and the use of an internal gear hub, partial fairings versus full body fairings, and adjustable riding elements such as handlebars and pedals. Design decisions regarding the incorporation of these features are addressed below in section "Concept Development and Selection Methods."

c. Prior Work

The only prior work used in the fabrication of this vehicle was the seat, which was taken from our 2011 vehicle. Our team made the decision to reutilize this feature because in our assessment of previous SPV vehicles, it was noted that the seat on last year's bike was uncomfortable and not suitable for long distance riding. In comparison, the custom upholstered, carbon fiber seat used on the 2011 vehicle was found to be comfortable, functional, and in good condition. We chose to not redesign the seat, but instead reuse this quality part so that we could focus our design efforts on the new, innovative aspects of our vehicle such as the full body fairing and the

suspension stabilization system. It is also important to note that the brackets used to attach the seat to the frame, as well as the incorporated safety belt system, are not included in "prior work." They are new designs that were made this year.

d. Design Specifications

In order to select design criterion for our bike, we created a list of fourteen requirements that we felt would be necessary for a high performance vehicle. From these fourteen requirements, we compared competition regulations and past team successes in order to emphasize certain requirements as being the most important. Based upon our House of Quality, which can be seen below, safety, stability, durability, innovation, and comfort were determined to be the most crucial design requirements for our bike. It can also be seen that we have targeted weak design areas from our previous bikes. Because maximum speed and drag reduction are the most prominent, we are seeking to improve on these aspects in the design of this year's vehicle by incorporating a full carbon fiber fairing. [2], [9], [10]

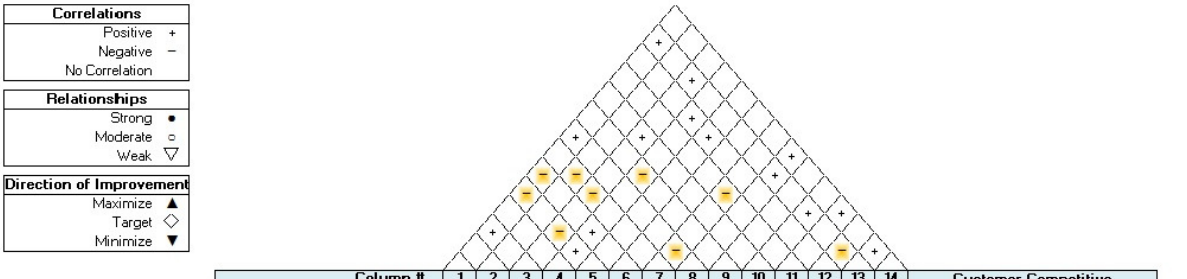

Row #	Weight Chart	Relative Weight	Customer Importance	Maximum Relationship	Team Requirements (Needs) \ Functional Requirements (Metrics)	1 Maximum Speed	2 Meets Factory of Safety Requirements	3 Minimize Weight	4 Failure During Competition	5 Potential Points of Contact	6 Small Turn Radius	7 Dollar Cost	8 Drag Force Reduction	9 Broken Components	10 Min. Size of Utility Compartment	11 # of New Designs	12 Comfortability	13 Minimal Volume	14 Attractive Appearance	Our Product	Competitor #1	Competitor #2	Row #
1	III	8%	7	9	High Speed	●	▽	●	▽	▽			●					▽		4	3	5	1
2	IIIII	10%	9	9	High Safety		●			▽	○	▽		●		▽				5	4	4	2
3	II	4%	4	9	Low Weight	●	▽	●	▽			▽			○	○		○		3	4	4	3
4	III	8%	7	9	Endurance				●											4	5	4	4
5	IIII	9%	8	9	Stability	○	▽	▽		●	○		▽		▽	▽		○		5	4	4	5
6	III	8%	7	9	Maneuverability	▽	○	○		○	●				▽	▽	○	○		4	4	4	6
7	II	4%	4	9	Low Cost			○				●	▽	○	▽	○		○		2	5	3	7
8	III	7%	6	9	Aerodynamic	○				▽		○	●		▽			○		4	4	5	8
9	IIII	9%	8	9	Durable		●					▽		●		▽				4	4	5	9
10	III	7%	6	9	Utility			○	○		○		▽		●	○		▽		3	4	3	10
11	IIII	9%	8	9	Innovative	▽	▽	○				▽				●				5	4	5	11
12	III	8%	7	9	Comfortable					○						●	●		●	4	4	5	12
13	II	4%	4	9	Practical Size	○		○		▽		▽	○		○	▽		●		3	4	5	13
14	II	4%	4	9	Aesthetics			▽		▽		○	▽		▽		●	○	●	3	4	3	14
					Max Relationship	9	9	9	9	9	9	9	9	9	9	9	9	9	9				
					Technical Importance Rating	189	226	222	103	162	148	111	170	185	120	239	135	166	111				
					Relative Weight	8%	10%	10%	5%	7%	6%	5%	7%	8%	5%	10%	6%	7%	5%				
					Weight Chart	≡	≡	≡	=	≡	≡	=	≡	≡	=	≡	=	≡	=				
					Previous Year	25	Y	63	N	3	25	5k	25	2	36	1	6	70k	7				
					Direction of Improvement	▲	◇	◇	◇	▲	▲	▼	▲	▲	▼	▲	▲	▼	◇				
					Target	40	Y	63	N	4	10	7k	50	0	18	2	8	80k	7				
					Units	40	Y/N	lbs	Y/N	tires	ft	$	%	#	in^3	#	#	in^3	#				

Figure 1: House of Quality

e. Concept Development and Selection Methods

Frame:

The design inspiration for the frame came from a multitude of sources ranging from concepts used by previous SPV teams to ideas found by researching current commercially available recumbent bikes. Before our initial concept development meeting, our team actually traveled to a recumbent cycling shop in Lexington, Oklahoma not only to get a feel for riding two wheeled recumbent bicycles, but also to gather ideas for our own designs. From our research and this field experience, our team determined that one of our chief goals was to design a comfortable bike suitable for riders of various sizes and riding abilities. Therefore, the spine of the bike was designed so the rider's center of gravity would be positioned as low as possible for ease of riding. Also, with regard to the aspect of safety, the roll cage was designed to withstand a 600 pound load while still protecting the rider in the event that they were to fall. For material selection, we considered aluminum, titanium, and steel, and found 4130 steel to be the most cost efficient, readily available/accessible, and most fundamental to weld. The aspect of being able to easily weld the material was a significant part of the material decision, because construction and sudden repairs could then be readily made to the frame using steel, whereas the other material options would require advanced expertise.

Fairing:

In an effort to increase the safety of our vehicle, considering the wide range of ability levels we were designing for, we decided to incorporate a full aerodynamic fairing into our design. The primary constraints we used to design our fairing included sizing, aerodynamics, and manufacturing. Sizing was the most important parameter of the fairing design because it is necessary to fit the frame and the rider inside of it completely and comfortably. Rather than cramming into the minimal amount of space possible, we decided to employ more of a club racer style fairing that allows for the rider to adjust their range of motion or posture during potentially lengthy rides. This resulted in a rather large design encapsulating the protective roll cage of our frame. Secondly, the fairing needed to retain an aerodynamic shape in order to remain competitive at the collegiate level. Generally, the most aerodynamically desirable design for a recumbent fairing is one which utilizes an airfoil shape from the top view and has a minimal amount of frontal area.

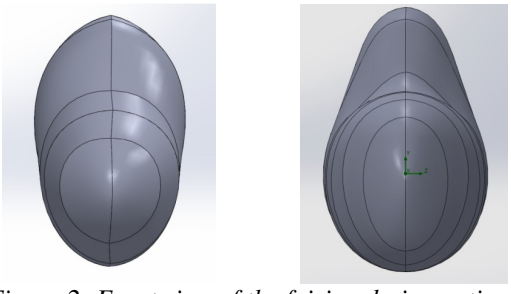

Figure 2: Front view of the fairing design options

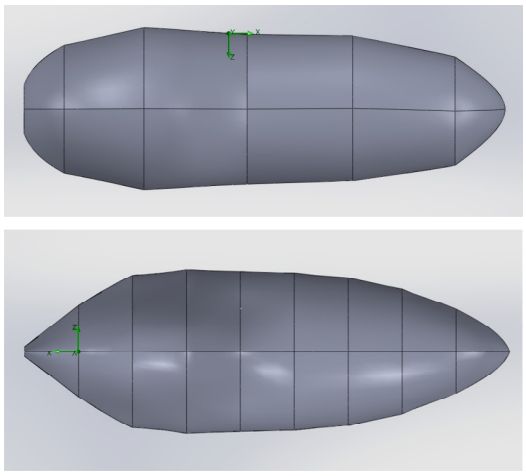

Figure 3: Top view of the fairing design options

Figures 2 and 3 above illustrate two different fairing designs that were considered for our bike. Because we were designing for the smallest frontal area and the most aerodynamic shape, the second design option was clearly the best choice. In addition to having smoother curvature, a smaller nosecone and window section, and a more progressive slope from the thickest to the thinnest point, the second design option also included a tail feature to assist with minimizing the stagnation and turbulence experienced on the back of the bike at high speeds. The second option was also effective at preventing flow separation along the length of the fairing, thus promoting a laminar flow and reducing the effects turbulent flow would have on balance and speed. Lastly, we wanted to ensure that our design would be feasible to manufacture. Due to the large size of our fairing, we were able to refrain from designing too many complex curvatures that could inhibit drape-ability or cause crimping issues with the composite material. The trade off we accounted for this generous fairing design was an increased amount of time spent on mold preparation and lay up, but because of the aforementioned benefits, this was justified.

In addition to developing the concept of the fairing shape, decisions had to be made regarding the type of composite material that should be used for fairing manufacturing. Because there is a wide array of possible choices for material, a significant amount of research had to be done to determine a suitable composite material to for our structural constituent. The primary material parameters and characteristics that were considered included: cost, weight, stiffness, toughness, impact resistance, and strength. Table 1 seen below was used as a Quality Function Deployment (QFD) matrix to sort out the benefits and consequences of different composite materials.

Table 1: Material Comparison Matrix [3]

Material Comparisons					
PROPERTY	**Best ----------> Worst**				
Cost	E-Glass	S-Glass	Kevlar	Carbon Fiber	Ceramic
Weight	Kevlar	Carbon Fiber	S-Glass	E-Glass	Ceramic
Stiffness	Carbon Fiber	Kevlar	S-Glass	Ceramic	E-Glass
Heat Resistance	Ceramic	S-Glass	E-Glass	Kevlar	Carbon Fiber
Toughness	Kevlar	S-Glass	E-Glass	Ceramic	Carbon Fiber
Impact Resist.	Kevlar	S-Glass	E-Glass	Ceramic	Carbon Fiber

Table 1 was used as a comparison matrix for commonly utilized composite materials [2]. It was seen that Kevlar had promising weight, toughness, and impact resistance characteristics, while

carbon fiber had promising weight and stiffness characteristics. Unfortunately, because carbon fiber becomes more stiff and brittle after introducing resin to the composite structure, it has weak toughness and impact resistance characteristics. Based upon these results, the optimal fairing choice was a combined use of Kevlar for impact and carbon fiber for structural strength. However, additional analysis was done to compare E-Glass and S-Glass because they also had moderate performance characteristics and at a better price. The ceramic composite was removed as a possibility based on our criterion.

Table 2: Mechanical Property Comparison Matrix [3]

Mechanical Property Comparison			
Property	**Aramid**	**Graphite/ Carbon**	**Fiberglass**
High Tensile Strength	B	A	B
High Tensile Modulus	B	A	C
High Compressive Strength	C	A	B
High Compressive Modulus	B	A	C
High Flexural Strength	C	A	B
High Flexural Modulus	B	A	C
High Impact Strength	A	C	B
High Interlaminar Shear Strength	B	A	A
High In-plane Shear Strength	B	A	A
Low Density	A	B	C
High Fatigue Resistance	B	A	C
High Fire Resistance	A	C	A
High Thermal Insulation	A	C	B
High Electric Insulation	B	C	A
Low Thermal Expansion	A	A	A
Low Cost	C	C	A

Using Table 2, we targeted the mechanical properties of the three different composites that we were considering; aramid fiber (Kevlar), carbon fiber, and fiberglass. The results of this analysis further solidified our predictions about using dual material consisting of carbon fiber as the primary structural constituent and with an incorporated aramid component for the critical impact points. Based on our findings and the techniques used by other successful teams, we decided to remove fiberglass as a possibility and incorporate Nomex honeycomb ribs for strength in critical locations on the fairing.

Having decided upon a primarily carbon fiber fairing, the next stage of the decision process required the selection of possible weave patterns, fiber orientations, and resin systems. In order to determine the most effective weave patterns for our application, a weave properties table was used to compare between satin, twill, plain, basket, and leno carbon fiber weaves.

Table 3: Carbon fiber weave style comparisons [15]

Weave Styles					
Properties	**Satin**	**Twill**	**Plain**	**Basket**	**Leno**
Good Stability	2	3	4	2	5
Good Drape	5	4	2	3	1
Low Porosity	5	4	3	2	1
Smoothness	5	3	2	2	1
Balance	2	4	4	4	2
Symmetrical	1	3	5	3	1
Low Crimp	5	3	2	2	2
Totals	25	24	22	18	13
5: Excellent 4:Good 3:Acceptable 2:Poor 1:Very Poor					

Using Table 3 above, we determined that plain weave or twill weave would be good weave orientations for our recumbent fairing application. Because stiffness and strength are desirable characteristics for a fairing, satin weave and basket weave were rejected because of their poor stability rating. Despite having excellent stability, the leno weave was rejected because of its poor and very poor ratings in all of the other categories. Twill weave and plain weave were seen to be the most balanced in terms of performance and manufacturability, and were therefore chosen as prime candidates for testing and further analysis.

Drivetrain:

For the drivetrain aspect of the vehicle, our main objective was to increase the speed potential of the bike while maintaining design that will eliminate misalignment issues that have caused trouble in past drivetrain designs of our team. For starters, we chose a chain and sprocket system over the belt driven system from past years, and we did this for several reasons.

Table 4: Decision Matrix of Belt Versus Chain Drivechain

	No Rust	No Lubricant	Simple Alignment	Easy Removal	Lightweight	Adjustable Length
Belt	YES	YES	NO	NO	YES	NO
Chain	NO	NO	YES	YES	NO	YES

Not only did our team want to be cost efficient with our design, but we foresaw the need to have a malleable chain line so we could easily thread the chain through our full fairing bike. In comparison, a belt driven system must remain perfectly straight between front and rear sprocket, which would be difficult to do around other features of our bike such as the landing gear. Additionally, a safety consideration was noted that a chain driven system would allow us to place a chain tube around the chain, thus eliminating the chance that clothing would be caught in the chain.

Pedaling System:

The design for the pedaling system was made with innovation, comfort, and stability in mind. The 2012 SPV team did not have an adjustable seat or pedaling system, which made it difficult for riders that were either shorter or taller than the average. After researching different variations of adjustable seats, most seemed to cause the center of mass to shift among the riders and potentially affect their balance. Therefore, we determined that by having an adjustable pedaling system the center of mass will be much more consistent for every rider, thus eliminating any concerns with balance. Our design will minimize the time between rotating drivers by using the quick-pin changing method, while still achieving an acceptable measure of comfort for any rider.

Landing Gear:

Similar selection methods were used with respect to developing a concept of a safe and innovative stabilization system for our full-fairing recumbent bicycle, otherwise referred to as landing gear. This design feature was deemed necessary in order to stabilize the vehicle as riders both begin pedaling and come to a stop. Various design concepts were initially tossed around for the landing gear design including a pneumatic suspension system and a telescopic landing system. However, two other concepts were more seriously considered under the basis of practicality and feasibility. The first was a simple rotating shaft that would attach to the back end of the bike frame. It can be seen in Figure 4 below, this design connected two legs to a shaft that

touch the ground at a 20° angle. The second design also consisted of a rotating shaft, but instead of two straight pipes for legs, it utilized two concentric tubes with a spring in the middle to incorporate suspension. This design can be seen below in Figure 5.

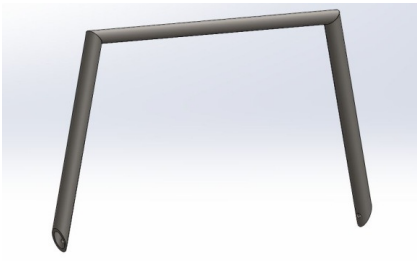

Figure 4: Rigid Legs

Figure 5: Suspension Based System

The second model was the design that was ultimately chosen specifically for its innovative suspension feature. It was concluded that not only would the suspension provide a smoother ride for the driver by absorbing shock, but it would also allow the driver to maneuver sharp turns more manageably as well. The springs used for the development of the landing gear prototype were standard compression springs, however, during this time an idea was brought forward to investigate variable springs, which would absorb some initial shock without reaching full compression until a substantially larger load was applied. Working with Cannon Spring Company in Oklahoma City, we concluded that a variable spring would better suit our landing gear application.

Additionally, because it is not ideal to weld springs directly onto metal plates, we needed to design a unique way to connect the legs of the suspension system to the frame, while also preventing them from twisting around when in the air or on the ground. The first choice was to drill holes into the plates and secure rope through the spring to tie the legs together, but the second, more sophisticated idea was to implement a pin and slot system onto the legs. To utilize the landing gear properly, a sliding mechanism was created to extend and retract the stabilization system. This mechanism is further explained in the "Description" section below, but it was chosen over a ring and cable method because the ring would have needed to be located somewhere near the chain, which may have caused interference and created a safety hazard. Lastly, there were several selections to choose from when deciding on the wheels for the landing gear. Multiple rollerblade and scooter wheels of various models and sizes were investigated, and ultimately the decision was made to use a 98 mm scooter wheel because it provided a wider wheel base and therefore more stability for the landing gear.

Steering:

This year, we wanted to design a steering system for the vehicle with high priority placed both on innovation and comfort to every member of our variously sized team. Because of the wide range of heights/arm lengths of the members of our team, it was decided that the best way to meet these ergonomic design goals was to make the steering and handlebar system easily adjustable. Not only would a rotating handle bar system allow each rider to personalize the steering placement for better vehicle control, but this design would also aid us in entering and exiting the vehicle by allowing riders to flip the handlebars out of the way of entry.

f. Innovation

Pedaling System:

The pedaling system is one of the unique features being built in to this year's bike. It was our design goal this year to create a bicycle that would be comfortable for all riders of different heights. While we have seen some recumbent bikes address this issue with adjustable seating, our team chose to design an innovative adjustable pedaling system. In our design, each rider will be able to move the pedals to a custom length, which will make the bicycle more functional for a wide variety of rider heights. Because commercial recumbent bicycle companies do not have adjustable pedaling systems of this nature, our design approach is distinctive. The unique slot system of our pedaling device will not only make it easier to rotate drivers during the race, but it will save time as well.

Landing Gear:

Nearly every two-wheel recumbent bicycle has some sort of landing gear or stabilization system, but our stabilization system is particularly unique because it incorporates a distinct suspension feature. By integrating suspension into our landing gear design, the riders of our bike will not only have a smoother ride, but they will more importantly have four wheels of safe contact on the ground while taking off, coming to a stop, and making difficult turns. Because the landing gear is made with concentric tubes, a system was needed to keep the tubes from twisting. This led to another innovated feature involving a pin and slot system, which prevents the pipes from rotating and from slipping off one another when the system is retracted into the fairing.

Steering:

One innovative concept regarding the steering design of the vehicle was the aforementioned adjustable handlebar stem. By implementing this adjustable stem, not only could riders easily maneuver their bodies in and out of the bike without interference from the handlebar, but they could also modify the position of the handlebar to fit their personal arm length needs. This feature is particularly innovative for the 2013 design team since it is our team's goal to increase our competitiveness at the collegiate level. Specifically, the swift exchange of riders that will be made possible with our adjustable handlebar system will aid us in the endurance category of the HPVC competition.

g. Description

Frame:

This year's team chose to go with a two-wheel recumbent bike in order to be more competitive in this year's competition. The ideas for the frame design came from observing last year's competition and previous teams' concepts. The new frame design allows us to have a durable and safe structure, as well as more relaxed seating for the rider. The frame of the bike is also designed to where all parts can be assembled with ease and goals of letting any rider, regardless of experience, control the bike. Basic design elements such as front wheel placement and steering shaft were taken from various commercial recumbent bicycles and applied to a conceptual CAD drawing as seen below.

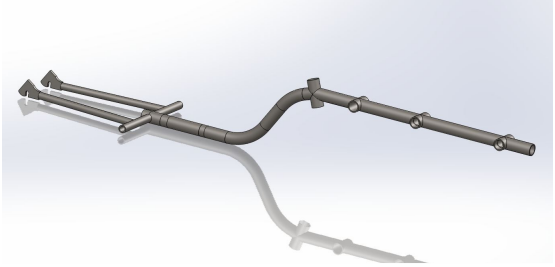

Figure 6: Basic Spine of Frame

The design process began with the general layout of the spine, positioning of the seat, pedal mount, and gearboxes in their intended locations. This gave the team basic dimensions and a place to start designing the rest of the bike. With a general layout of the spine, various support systems for holding the bike up started to be designed along with more important features such as the roll cage, steering, and pedaling system. With these features and wheel layout selected, the frame went into development.

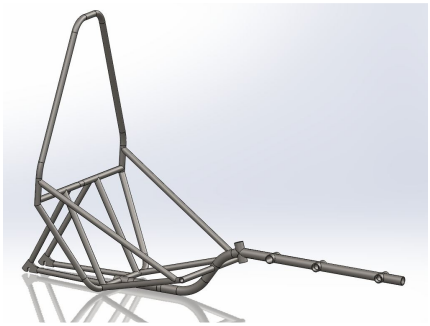

Figure 7: Full Frame

When designing the roll cage, measurements of our tallest rider were taken to ensure that the driver's head would still remain within the boundary of the roll cage in the event of a fall. The next concern was how to protect the arms and body of the rider if falling over was to occur. A side rail running the length of the cabin portion of the frame was designed to make contact with the ground well before the rider's body, absorbing the impact force and protecting him/her during a fall. This particular frame meets our design goals of safety and durability.

Other components of the frame such as the back wheel dropouts and the front steering column were designed around a comfortable seating position for the rider. In order to allow the rider to sit up and not pedal at an incline, the front wheel was placed where it will not interfere with the pedal when in motion. This resulted in positioning the front wheel as close to the spine as possible. Maintaining a fork angle of 20 degrees was also very important because it allowed the bike to be easily maneuverable for the exchange of riders. The back wheel was positioned to be as close to the back of the seat as possible in order to make ground contact with the same horizontal plane as the front wheel.

Drivetrain:

An additional aspect of the vehicle design that was considered was the gear design of the drivetrain system. On the 2012 SPV vehicle, the team used a 14-speed internal planetary gear hub in their drivetrain design, but the team experienced many problems from the chain slipping

at the competition. Upon further inspection, it was found that the gear hub had been improperly installed; the mounting brackets had been improperly secured to the frame. Because the internal gear hub is a very powerful and rather expensive drivetrain element, our team decided that it would be advantageous to reincorporate it into our new vehicle design, assuring that it was installed and used properly.

With this aspect of the drivetrain established, our next step in drivetrain design was centered around our team's desire to increase the gear ratio, and therefore the speed potential, from the previous year's gear ratio of 4.5. Because we had already made the decision to utilize the powerful 14-speed internal gear up that our team already owned, we knew that the rear gear should be a threaded 16 tooth sprocket. Therefore, to increase the gear ratio without using an impractically sized front sprocket (80+ teeth), we chose to design a two-stage drivetrain system. While the front and rear sprockets of this dual stage system were attached either by the crankset or the gear hub, individual spiders were necessary to attach the two sprockets in the center of the chain line to their respective bottom bracket shafts. Isolated spiders are not common in the bicycle market except for a handful of expensive proprietary parts that would require the drivetrain to be redesigned around an entire customized system of spiders and bottom brackets. To remain cost efficient, the decision was made to design and fabricate custom spiders for the vehicle.

Figure 8: 20-tooth Sprocket with Custom Made Isolated Spider

The spiders for this drivetrain system were designed using SolidWorks 2012, and the dimensioning of the parts was guided mainly by the bolt-hole patterns of the sprockets and the shaft measurements of the bottom bracket they attach to. In order to keep stress concentrations to a minimum, sharp corners were avoided where possible. The rest of the spider features were chosen to optimize the strength-to-weight ratio and fatigue lifespan.

Pedaling System:

The innovative pedaling system was designed to accommodate various heights for the riders without changing the dynamics and performance of the bike. The idea was to keep the center of mass the same for all riders and simply adjust the pedals for people with shorter or longer legs. This would eliminate concerns about maintaining consistent stroke radius for each rider while keeping human fatigue the same. The concept to have two separate pedaling cranks with a bracket connecting them can be seen in the CAD design below.

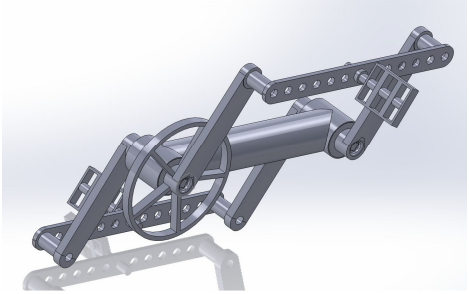

Figure 9: Adjustable Pedaling System

Once the initial design concept was decided upon, more elaborate details such as how the pedal would move from one position to another were further developed. Initially a push button was designed to hold the pedal into the desired position, however, fabricating such an intricate design proved to be an extremely difficult task to complete in a timely manner. Therefore, a redesign of the locking mechanism was created and would not only be easier to fabricate, but would also prove to be a better overall design with more security in the system to ensure the pedal does not come free.

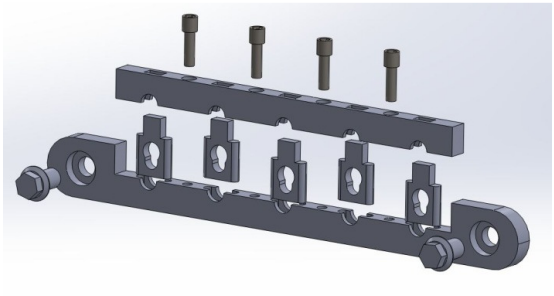

Figure 10: Initial Locking Mechanism

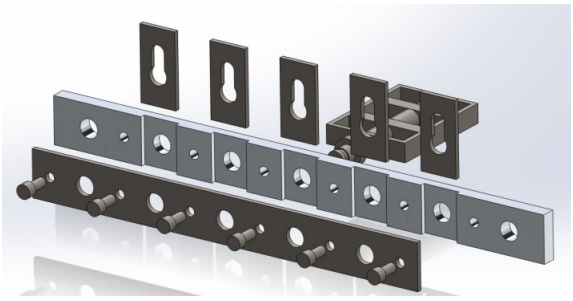

Figure 11: Final Locking Mechanism

With the final bracket designed and the overall concept ready to be put into production, some proof of concept work was needed. First a CAD assembly was created with all the parts involved, which worked well in the program. Second, two different crank systems were attached to ensure everything would fall into place. Third, a prototype bracket was fabricated to prove the concept of locking the pedals into place using a slide could be done.

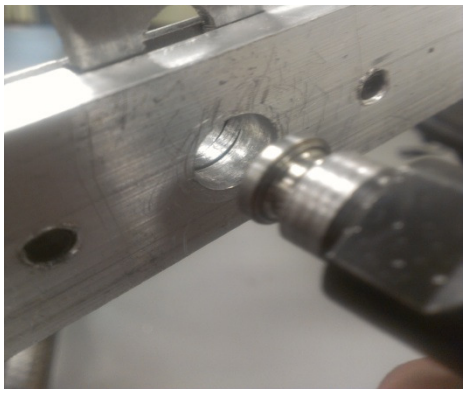

Figure 12: Pedal and Locking Prototype

Figure 13: Pedal Locked in Place

With all the separate pieces fabricated, the final prototype was created and assembled. Given the large open area the bike has in front, where the pedals would be, this made it a very easy to adapt into the final design.

Landing Gear:
The main purpose of the landing gear is to stabilize the recumbent bike at slow speeds or a complete stop. The landing gear will act like training wheels at low speeds, but will retract once the rider begins operating the recumbent bike at a faster pace. Connected to the shaft are two concentric tubes that touch the ground at a 20° angle and have springs lodged between two plates to act as suspension. Below is a computer aided design (CAD) model of the design.

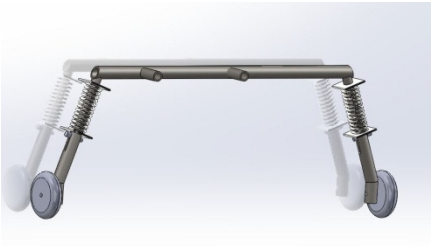

Figure 14: Suspension Based System

The purpose of the suspension system is to provide a smoother ride for the driver by absorbing shock and allow him or her to maneuver sharp turns at slow speeds. To absorb shock, we needed to design a spring suspension system, so we contacted a local business called Cannon Spring Company to discuss possible springs. Upon hearing what we needed, Cannon Spring offered to make custom springs with variable spring constants for our use. These variable springs increase in stiffness as the compression increases, thus stiffening the springs as needed.

The landing gear is controlled by a sliding mechanism attached to the right shoulder bar of the recumbent bike. The stabilization system could then extend and retract using a cable attached between a pivot pipe, located on the landing gear, and the sliding mechanism. In order to keep the landing gear extended, the rider simply hooks the sliding mechanism to a fixed shaft attached at the other end of the bar as seen in figure 15 below.

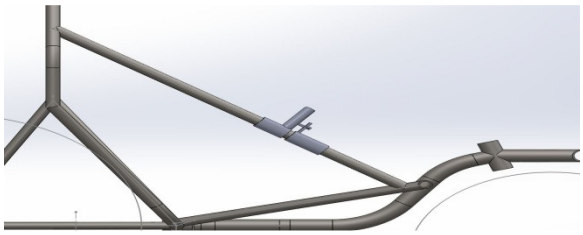

Figure 15: Sliding Connection Mechanism

To prevent the landing gear from going too far forward, a stop was created below the spine of the frame. The stop is made out of a steel plate and has two notches cut on opposite sides to fit both the spine and a prevention pipe, which is also located on the landing gear.

In order to keep the landing gear retracted, a common utility spring, which can be purchased at any local hardware store, was added to hold the system up as the rider kept the bike in motion. Below is a figure showing the retractable spring concept.

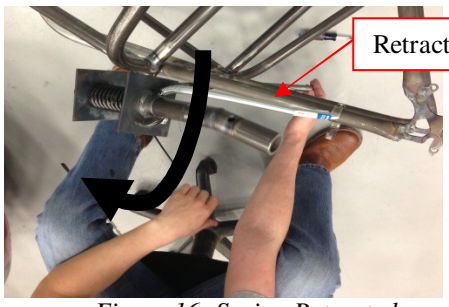

Figure 16: Spring Retracted

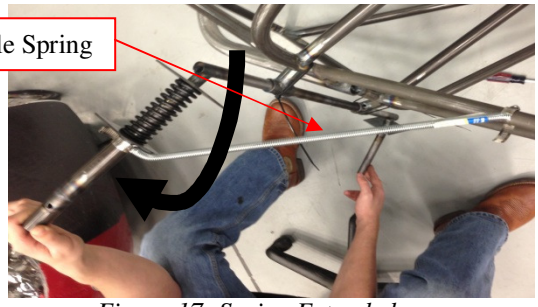

Figure 17: Spring Extended

Because it is not ideal to weld the springs onto the plates, a system was needed in order to prevent the concentric tubes from rotating and slipping off. The method of the choice to prevent the legs from rotating was a pin and slot system. The pin and slot system, another new feature, works by drilling a hole into the smaller pipes and slots in the larger ones. This system will not only prevent the legs from rotating, but it will also allow the legs to properly compress with the springs and stop the legs from slipping off one another as the system retracts into the fairing. Below are two figures showing the showing the pin and slot method as it is being compressed and standing at free height.

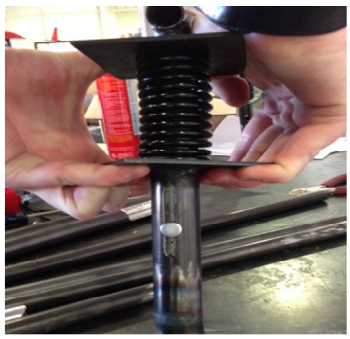

Figure 18: Pin and Slot Compressed

Figure 19: Pin and Slot at Free Height

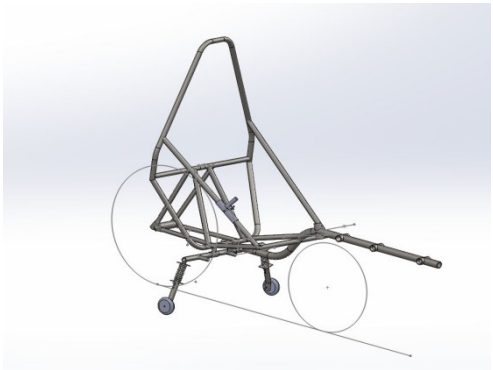

Figure 20: Landing Gear/ Bike Assembly

Steering:

The steering portion of the bicycle was designed to be as lightweight as possible, while still placing high priority on functionality and comfort for the rider. A crucial aspect of the steering design was the head tube angle, as shown below [16], because the head tube angle is essential for skillful handling of the bike.

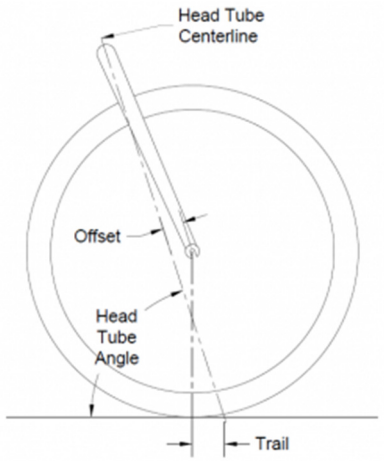

Figure 21: Diagram of Head Tube Angle

Multiple criteria were taken into account when designing the head tube angle, which include having a competitive turning radius, avoiding heel overlap, and avoiding hitting the rider's legs during a sharp turn. The design team decided on a relatively conventional 70° head tube angle to satisfy these criteria.

Ergonomics were also considered during the design of the steering system. Because our SPV team varies greatly in height, an adjustable handlebar system was of high importance both for the ability to control the vehicle comfortably as well as the ability to exchange riders without handlebar interference. By using a handlebar stem with an adjustable angle, we will be allowed to personalize its placement and fold it completely out of the way during rider exchange. Additionally, ergonomic grips were acquired to comfortably fit in the rider's hands, providing a more enjoyable riding experience overall.



Figures 22, 23, 24: Display of Adjustable Handlebar Stem Angle

Analysis

a. RPS Analysis

In accordance with the rules for the 2013 HPVC, the design team analyzed two static cases of roll cage loading with ANSYS Workbench 14. The first loading case is a 300 lb. load applied horizontally to the roll bar at the rider's shoulder height, which simulates the vehicle in a side crash. As instructed by HPVC rules, the horizontal load is reacted by fixed constraints of where the vehicle seat would be attached to the frame. The results of this analysis can be seen in the figure below.

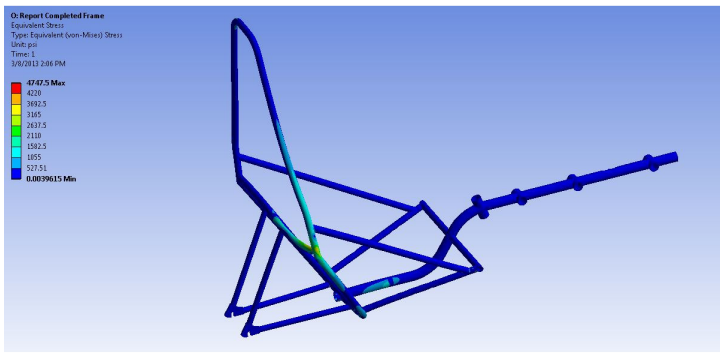

Figure 25: Von-Mises Stress due to 300 lb Horizontal Load on RPS

From this analysis, the design team found that the maximum von-Mises equivalent stress acting upon the right shoulder side of the roll cage was 4747.5 psi. When compared to the yield strength of 4130 steel (63300 psi), a safety factor of 13.33 is calculated and assures the rider that a side crash would not cause the rollover protection system to fail. In addition, the total elastic deformation due to the horizontal loading was calculated to be 0.0123 inches, which is much less than the allowable 1.5 inch deformation standard set by HPVC rules. This ensures the design team that in the event of a side crash, the rollover protection system will not deform such that contact with the driver's helmet or head will occur. Therefore, the design team is confident that the rollover protection system will meet the safety rating and protect the rider in the event of a side crash.

The next static loading case that was performed on the rollover protection system was a 600 lb. vertical load acting downward at the top of the roll bar at a 12 degree angle from the vertical. As instructed by HPVC rules, the vertical load is reacted by fixed constraints of where the vehicle seat would be attached to the frame. The results of this analysis can be seen in the figure below.

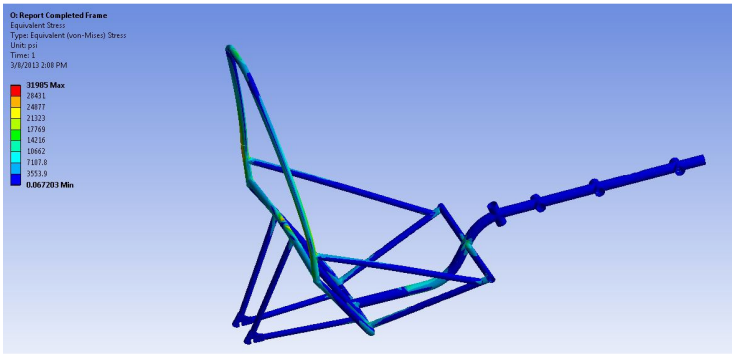

Figure 26: Von-Mises Stress due to 600 lb Vertical Load on RPS

From this analysis, the design team found that the maximum von-Mises equivalent stress acting upon the roll cage was 31985 psi. When compared to the yield strength of 4130 steel (63300 psi), a safety factor of 2.0 is calculated and assures the rider that if the bike were to flip over, the rollover protection system would not fail and keep the rider safe. In addition, the total elastic deformation due to the vertical loading was calculated to be 0.7 inches, which is much less than the allowable 2 inch deformation standard set by HPVC rules. This ensures the design team that in the event of the vehicle flipping, the rollover protection system will not deform such that contact with the driver's helmet, head, or body will occur. Therefore, the design team is confident that the rollover protection system will meet the safety rating and protect the rider in the event that the vehicle flips over.

b. Structural Analysis

In order to analyze the structural strength of the frame, the design team wanted to confirm that the frame geometry would be able to withstand the weight of the team's heaviest rider, which weighs in at close to 200 lbs. Using ANSYS Workbench 14, the design team simulated the resulting stress that the bike would experience under a 200 lb. loading acting on the spine of the frame where the bottom of the seat would attach to the frame. For the highest level of accuracy, the design team used fixed constraints where both the front and rear tire would attach to the frame. The results of this analysis can be seen in the figure below.

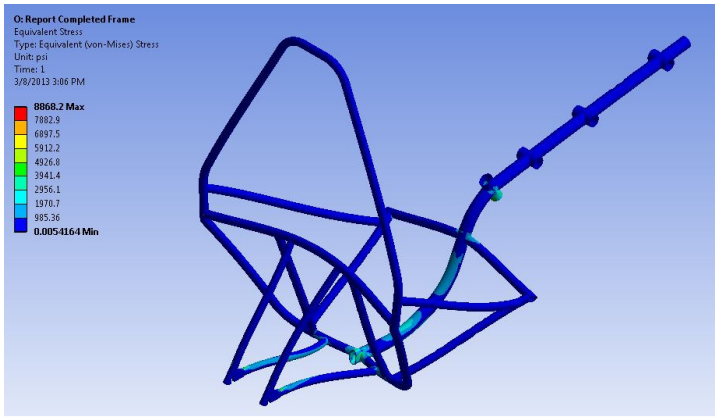

Figure 27: Von-Mises Stress due to Weight of the Rider on the Frame

From this analysis, the design team found that the maximum von-Mises equivalent stress acting upon the frame of the vehicle was 8868.2 psi. When compared to the yield strength of 4130 steel (63300 psi), a safety factor of 7.14 is calculated. In addition, the total elastic deformation due to the weight of the heaviest rider on the team was calculated to be 0.0071 inches. With such a high safety factor and extremely low deformation caused by the weight of the rider, the design team is assured that the frame will be more than capable to withstand the weight of each member of the team that will ride the vehicle during the competition.

c. Aerodynamic Analyses

In order to substantiate that our fairing design adequately reduced drag forces on the bike, SolidWorks Flow Simulation 2012 was used to perform CFD analysis and calculate the drag forces that the fairing would experience at different speeds. By performing the flow simulation at 5, 10, 15, 20, 25, 30, and 35 mph, the full range of bicycle operation could be considered and

evaluated against the option of not having a fairing or aerodynamic device. Table 5 below includes the results of the seven flow simulations mentioned above. At each speed, the drag force was set as a global goal for the simulation so that it would quantify the global drag force experienced on the bike.

Table 5: CFD Simulation Results for a direct frontal flow

Run	Frame w/ Fairing		Frame	
	Drag Force (lb)	$C_DA\ (ft^2)$	Drag Force (lb)	$C_DA\ (ft^2)$
5 mph	0.134	2.096	0.213	3.328
10 mph	0.412	1.612	0.842	3.295
15 mph	0.947	1.646	1.900	3.303
20 mph	1.665	1.628	3.375	3.300
25 mph	2.585	1.618	5.287	3.309
30 mph	3.729	1.620	7.606	3.306
35 mph	5.053	1.613	10.339	3.301

By using the fundamental equation for drag force (1) and the average air density at sea level, the C_DA could be calculated to signify the total effective frontal area that experiences the drag by using equation (2).

$$F_D = \left(\frac{\rho}{2}\right) V^2 C_d A \tag{1}$$

$$C_dA = \frac{2F_D}{\rho V^2} \tag{2}$$

Because the angle of flow and direction of flow did not change for the direct frontal flow simulations, C_DA should remain roughly constant if the simulation is accurate. It can be seen in our data that the ratio of the drag force to the flow velocity squared is roughly the same for each simulation, producing the desired constant C_DA.

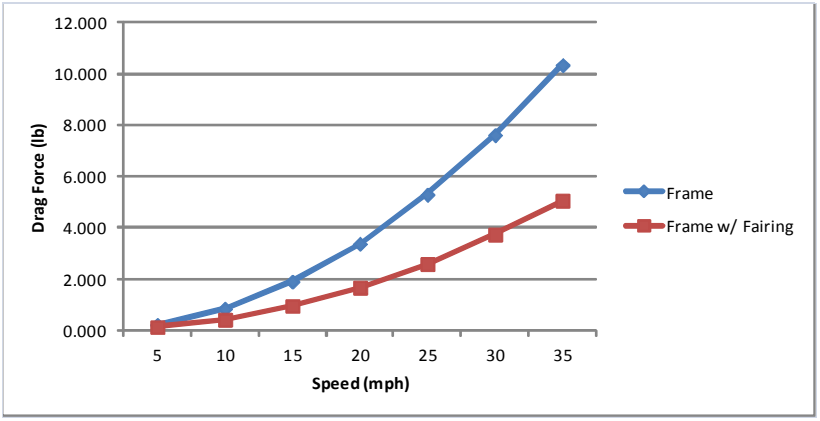

Figure 28: Graphical representation of the CFD drag comparison between fairing and no fairing options

Figure 28 illustrates the trend of the drag force with respect to vehicle velocity for the solo frame option, as well as the frame and fairing combination. It can be seen that the fairing effectively reduces the drag force experienced by approximately 50% at every operating speed. As the speed

increases, that 50% reduction becomes more and more significant, while at low speeds it becomes inconsequential.

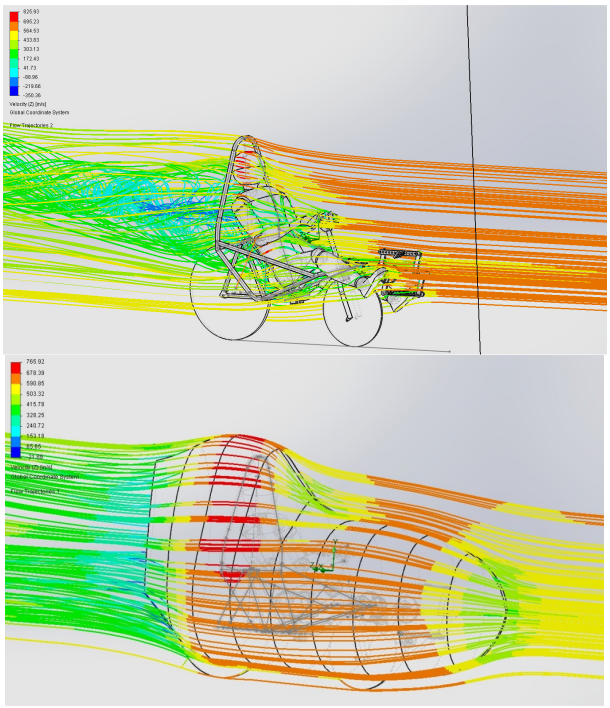

Figure 29: Flow trajectories for the frame and fairing options at 35 mph

Figure 29 illustrates the flow trajectories of air around the frame option (top) and the frame with fairing option (bottom) at a projected maximum speed of 35 mph (616 in/s). Because of the large contoured sides and streamlined shape of the fairing, there is a noticeable reduction in the turbulence of the air coming off of the tail section when compared to the obvious turbulence of the no fairing option. Without the fairing, the frame and human body create too sudden of a pressure differential for the boundaries layers of the air to remain laminar, thus creating a large stagnation point and turbulent vortices directly behind the rider.

In order to simulate a more realistic flow trajectory and operating condition, cross-flow analysis was taken into consideration. According to the National Climate Data Center, the average wind speed for the San Francisco Bay area for the past 75 years has been 12.2 mph (214.72 in/s) for the month of April [1]. Therefore, we simulated the worst case scenario of the average 12.2 mph being directly perpendicular to our fairing in combination with the seven direct frontal flow velocities that represent our potential vehicle speed. Table 6 below shows the results of the cross-flow analysis, including the resultant drag force and the effective area experiencing that force, $C_D A$, created by the combination of the flows.

Table 6: Cross-flow Analysis Results

Crossflow Analysis			
Run		Resultant Drag Force (lb)	$C_D A\ (ft^2)$
12.2 mph Cross Flow(Average windspeed of San Francisco Bay area in April)	5 mph	9.454	21.271
	10 mph	10.969	17.241
	15 mph	12.989	13.590
	20 mph	15.076	10.744
	25 mph	16.467	8.323
	30 mph	17.249	6.433
	35 mph	20.232	5.760

It can be seen that the drag forces and the area experiencing the drag are much higher for the cross-flow than they were for the direct frontal flow. This is primarily due to the fact that the fairing is large and less aerodynamic from the side. However, the data also shows that as the frontal flow becomes the primary flow, the effective drag force area and drag coefficient get smaller as the resultant air flow angle is changing and affecting a slightly different shape at each speed.

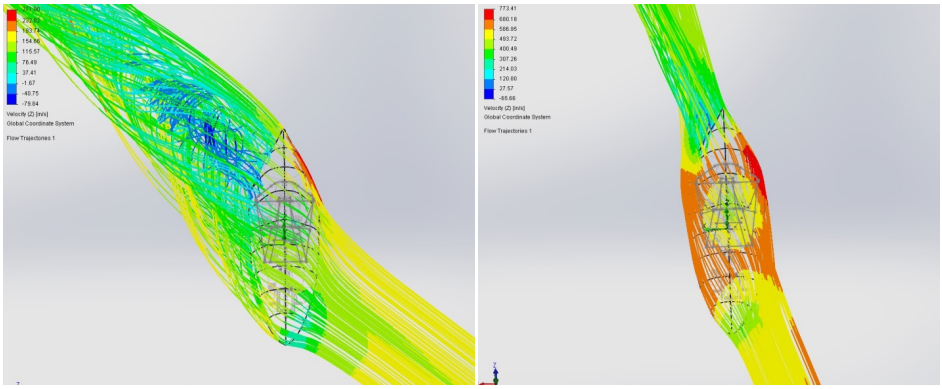

Figure 30: 12.2 mph side/5 mph front cross-flow trajectory (left), 12.2 mph side/35 mph front cross-flow trajectory (right)

Figure 30 illustrates the difference between the minimal frontal flow of 5 mph with the side flow of 12.2 mph (left) and the maximum frontal flow of 35 mph with the same side flow of 12.2 mph (right). Despite the velocity, and subsequent drag force, being larger for the maximum operating conditions, the flow characteristics show significantly less stagnation and turbulence in the resulting flow because the 35 mph front wind more effectively counteracted the 12.2 mph side flow and retained the air boundary layers along the sides of the fairing. Unfortunately, if we are faced with a direct perpendicular flow of more than 10 mph, it could be difficult to remain steady and balanced at low speeds. However, the use of a landing gear mechanism would allow for additional stability at low or take-off speeds when required.

d. Cost Analysis

Cost analysis of our vehicle was performed, and this year the vehicle was able to be manufactured at a total of $7,381. Additionally, we calculated the costs associated with manufacturing 10 of these vehicles per month for the next 3 years which came to a total of $1,682,487. This figure is including capitol costs, labor, materials, and overhead. When profits

from selling the vehicles are considered, we estimated that we would gain $477,512. The breakdown of allocations can be viewed in the figure below. [6], [7], [8], [12], [14]

Competition Vehicle Cost Estimation				
Description	Quantity	Unit Cost	Units	Total
Frame				
Frame Metal	26	$18.90	Per Feet	$491.51
Landing Gear Metal	4	$4.66	Per Feet	$18.62
Pedal Bearings	1	$26.58	Per Package	$26.58
Landing Gear Wheels	1	$20.00	Lump Sum	$20.00
Seat Brackets	2	In-Stock	Lump Sum	-
Seat	1	In-Stock	Lump Sum	-
Springs	2	Donation	Lump Sum	-
			Subtotal	**$556.71**
Fairing				
Mold	1	$4,999.00	Lump Sum	$4,999.00
Carbon Fiber	25	Donation	Per Yard	-
Epoxy Resin System	2	$170.00	Per Gallon	$340.00
Fiberglass Resin	2	$25.00	Per Gallon	$50.00
Nomex Honeycomb	24	Donation	Square Feet	-
Peel Ply	20	$8.95	Per Yard	$178.95
Release Film	20	$6.75	Per Yard	$134.95
Bleeder Cloth	20	$5.25	Per Yard	$104.95
Vacuum Bag	10	In-Stock	Per Yard	-
Vacuum Pump	1	In-Stock	Lump Sum	-
Tacky Tape	5	In-Stock	Per Roll	-
Assorted Tools	1	$50.00	Lump Sum	$50.00
			Subtotal	**$5,857.85**
Steering				
Fork	1	$140.00	Lump Sum	$140.00
Adjustable Stem	1	$70.00	Lump Sum	$70.00
Clamp	1	$10.00	Lump Sum	$10.00
Headset	1	$30.00	Lump Sum	$30.00
Handlebar Grips	1	$25.00	Lump Sum	$25.00
Handlebar Metal	4	$7.09	Per Foot	$28.35
Front Wheel	1	$225.00	Lump Sum	$225.00
			Subtotal	**$528.35**
Drivetrain				
Sprockets	3	$31.10	Lump Sum	93.31
Brackets	3	$37.98	Lump Sum	$113.93
Brakes	1	$94.79	Lump Sum	$94.79
Rear Wheel/Hub	1	In-Stock	Lump Sum	-
Chain	3	$20.00	Per Box	$60.00
Pedals	2	$20.00	Lump Sum	$40.00
Rear Wheel Tire	1	$37.00	Lump Sum	$37.00
			Subtotal	**$439.03**
			TOTAL	**$7,381.94**

Production Run Cost Estimation (3 years, 10 bikes per month)				
Description	Quantity	Unit Cost	Units	3-Year Total
Capital Investments				
Fairing Mold	1	$10,000.00	Lump Sum	$10,000.00
Mill	1	$22,000.00	Installments	$22,000.00
Frame Jig	1	$200.00	Lump Sum	$200.00
TIG Welder	1	$3,500.00	Lump Sum	$3,500.00
Band Saw	1	$2,000.00	Lump Sum	$2,000.00
Grinder	1	$200.00	Lump Sum	$200.00
Notching Machine	1	$1,075.00	Lump Sum	$1,075.00
Pipe Bender	1	$325.50	Lump Sum	$325.50
Lathe	1	$20,000.00	Installments	$20,000.00
			Subtotal	**$59,300.50**
Tooling				
Mill	1	$22,000.00	Installments	$22,000.00
TIG Welder	1	$3,500.00	Lump Sum	$3,500.00
Band Saw	1	$2,000.00	Lump Sum	$2,000.00
Grinder	1	$200.00	Lump Sum	$200.00
Notching Machine	1	$1,075.00	Lump Sum	$1,075.00
Pipe Bender	1	$325.50	Lump Sum	$325.50
Lathe	1	$20,000.00	Installments	$20,000.00
			Subtotal	**$49,100.50**
Parts and Materials (without donations or in-stock items)				
Cost Savings for Bulk Purchasing				20%
Drivetrain	360	$351.22	Per Bike	$126,440.64
Fairing	360	$1,727.08	Per Bike	$621,748.80
Steering	360	$422.68	Per Bike	$152,164.80
Frame	360	$545.37	Per Bike	$196,332.48
			Subtotal	**$1,096,686.72**
Labor				
Machinist/Welder	3	$1,600.00	Bi-Monthly	$115,200.00
Composite Tech.	3	$1,250.00	Bi-Monthly	$90,000.00
Floor Worker	4	$800.00	Bi-Monthly	$57,600.00
Manager	1	$2,400.00	Bi-Monthly	$172,800.00
			Subtotal	**$435,600.00**
Overhead Costs				
Building Rental	1	$2,000.00	Per Month	$72,000.00
Utilities	-	$500.00	Per Month	$18,000.00
Welder Operating Costs	-	$25.00	Per Month	$900.00
			Subtotal	**$90,900.00**
			TOTAL	**$1,682,487.22**
			Consumer Purchase Cost	**$6,000.00**
			Total Profit	**$477,512.78**

Figure 31: Cost Analysis for 2013 Vehicle

e. Other Analyses

Drivetrain:

In order to verify the durability of our sprockets, we chose to simulate the load that our largest 6061-T6 aluminum sprocket experiences when a rider places their maximum force on the drivetrain. Through research, it was found that the Japanese Industrial Standards (JIS) hold the most stringent safety requirements for bicycle manufacturing, stating that a crankset must withstand a static load of 337 lb. applied vertically to the pedal [11]. Since the crank length is 6.5 inches, the torque applied to the sprocket at maximum force is calculated to be 2190.5 in.-lbs, which correlates to a tension of 572.68 lbs. in the chain. Referencing the Standard Handbook of

Chains [5], the following two equations were used to determine the force distribution on each tooth of the 48 tooth sprocket

$$P_1 = t_1 \frac{\sin\alpha}{sin\varphi} = t_0 \frac{\sin\alpha}{\sin(\alpha+\varphi)} \quad (3)$$

$$P_n = t_n \frac{\sin\alpha}{\sin\varphi} = t_0 \left[\frac{\sin\alpha}{\sin(\alpha+\varphi)}\right]^{n-1} \left[\frac{\sin\alpha}{\sin\alpha+\varphi}\right] \quad (4)$$

where P is total force acting upon a single tooth, t is tangential force upon a single tooth, α is pitch angle of the sprocket, and φ is the pressure angle for a new chain. After determining the forces acting on the individual teeth, the sprocket was loaded using ANSYS Workbench 14 in the manner shown in Figure 32.

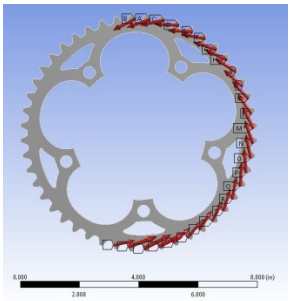

Figure 32: Loading Placed on Individual Teeth

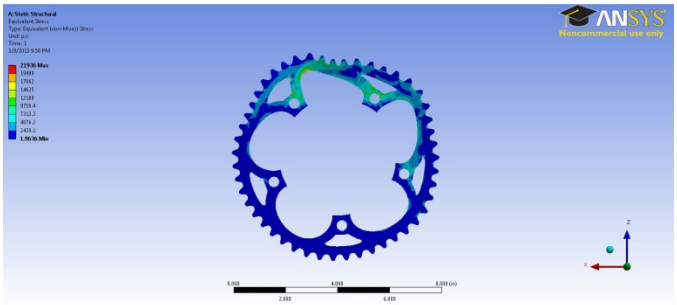

Figure 33: Von-Mises Stress Results on Sprocket

As shown in Figure 33, the maximum stress experienced by the sprocket was 12,637 psi, resulting in a safety factor of 1.74, verifying that the sprocket satisfies the requirements set by JIS and will be suitable for use in the drivetrain of our vehicle.

Pedaling System:

In order to verify that the pedaling system and bracket would not fail under expected load conditions, finite element analysis was used on both concepts. Using the heaviest expected weight of a rider and applying it as the force on top of the pedal, while constraining the bracket, we can see below that our pedal system should not fail. However, we do not expect a force anywhere near this magnitude to occur at any given time, and therefore we are satisfied with the results of the analysis. We also conclude that the system is no weaker than a normal pedal crank setup because the highest stress is located internally in the pedal shaft, the same location it would be on a standard crank setup, assuming the same loading situation, the stresses would be the same. FEA images of the pedaling system analysis can be seen in figures in 34 and 35 below.

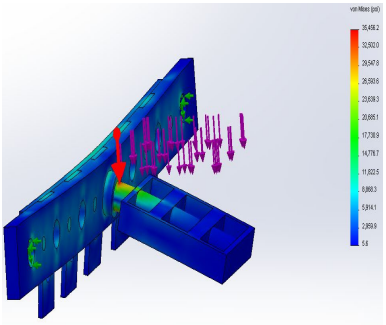

Figure 34: Von-Mises Stress on Pedal

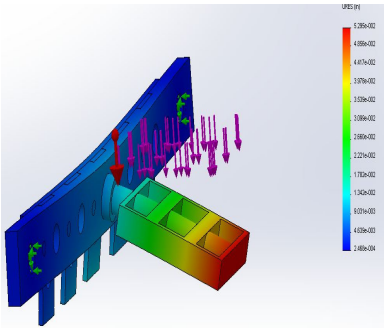

Figure 35: Deformation of Pedal

Landing Gear - Pivot Pipe:

When initially analyzing the landing gear system, the design team first had to determine what wall thickness of the 4130 steel piping used for the pivot pipe would prevent the pivot pipe from bending and ultimately causing the landing gear system to fail. Under normal operating conditions, the design team made the assumption that the maximum load acting upon the pivot pipe would be the total weight of the bike and the driver (280 lbs.) dispersed evenly between the two weld points. That is, each side of the pivot pipe would experience exactly half of the total weight of the bike and the driver, or 140 lbs. After testing multiple variations of different wall thicknesses using ANSYS Workbench 14, a final value of 1/8 inches was determined to be the most applicable to the vehicle's needs. The results of the finite element analyses performed using this particular wall thickness are shown below.

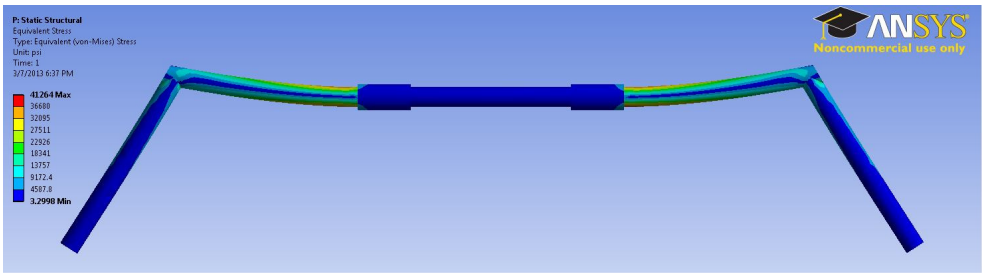

Figure 36: Von-Mises Stress due Vertical Loading on Landing Gear Pivot Pipe

It was found that a maximum von-Mises stress of 41264 psi and a maximum shear stress of 22434 psi are experienced by the pivot pipe. Using 63.3 ksi for the yield strength and 36.714 ksi for the shear strength of 4130 steel, the pivot pipe has an overall safety factor of 1.53 for the von-Mises equivalent stress and 1.64 for the shear stress. These safety factors are satisfactory and assure the driver that even if the pivot pipe experiences the total weight of the bike and the driver, the pivot pipe will not fail and will keep the driver from wrecking the vehicle.

Landing Gear - Horizontal Force:

Additionally, the design team had to determine the amount of stress acting upon the landing gear legs if they were to experience any horizontal loading due to potential uneven terrain. For this analysis, the design team assumed that the maximum horizontal force that would act upon one of the legs of the landing gear would be due to the leg running into a bump or falling into a hole at slow speeds. Since the landing gear would only be in contact with the ground at speeds between 0 and 10 MPH (14.67 ft/s), the design team measured the average acceleration of the team's fastest rider from those two speeds, which resulted in a value of 3.997 ft/s^2. Multiplying this

value with the mass of the bike (8.7 slugs), a resulting 34.78 lb. force was calculated as the maximum total force that would be applied to the end of one of the landing gear legs due to the vehicle colliding with a bump or falling into a hole.

Using ANSYS Workbench 14, this load was applied to a simplified model of a landing gear arm. It was assumed that any force acting upon the landing gear arm would transfer to the section of the leg that is at a 20 degree angle. Therefore, the design team was able to neglect the 3 inch section of the large pipe that the wheel attaches to and apply the 34.78 lb. load directly on the part of the larger pipe that is at a 20 degree angle. In addition, the section of the smaller pipe that is welded to the pivot pipe was fixed since the weld restricts all degrees of freedom of the top of the smaller pipe.

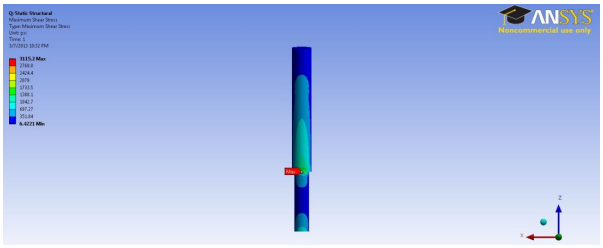

Figure 37: Von-Mises Stress due to Horizontal Loading on the Landing Gear Arm

The maximum von-Mises stress and shear stress acting upon the landing gear leg were found to be 5620 psi and 3115.2 psi, respectively. Using 63.3 ksi and 37.71 ksi for the yield strength and the shear strength of 4130 steel, respectively, results in a safety factor of 11.26 for the von-Mises stress and 11.79 for the shear stress. These safety factors assure the rider that if the vehicle were to experience any horizontal loading due to uneven terrain, the landing gear arms would not fail and would continue to balance the rider as expected.

Steering:

Finite Element Analysis (FEA) was performed on the handlebars and the stem of the vehicle to ensure that the design would not fail under normal conditions. This analysis was performed using several different wall thicknesses until the factor of safety was in a reasonable range. The FEA was conducted for this component under the following conditions: the base of the stem was fixed and the portion of the handlebars where the grips are located was given a moment of 50 ft-lb about the stem. The results are shown below.

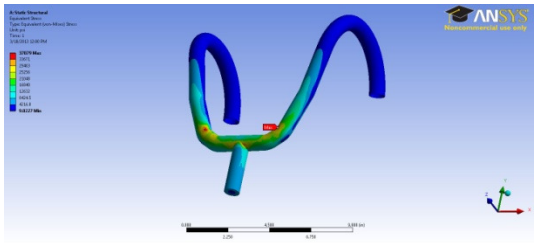

Figure 38: FEA on Handlebars, Von Mises Stress Results

As seen above, at the specified conditions, the handlebars experience a maximum stress of 37,879 psi. Since we were using AISI 4130 Steel, a material with a yield strength of 63,300 psi, it is seen that our handlebars have a safety factor of 1.67. Because we do not intend to exert this much force on our handlebars, they are considered durable and safe for use.

Testing

a. RPS Testing

In order to verify the calculated FEA results, we preformed two separate tests to simulate the loading conditions constructed in FEA. The first test was conducted by tilting the entire frame backwards at an angle of twelve degrees and firmly supported. Once the frame was in place a rope was attached to the top of the RPS and 200 pounds was asserted directly downward. This accurately simulated the FEA calculations and gave a total displacement of 0.25 inches which is accurate and linear to the relationship of the FEA calculation of 0.76 inches of displacement with a 600 pound load. With the top load scenario accurately tested the side load was preformed next. The bike was supported along the spine and held sideways. While in this position a 300 pound load was applied to the widest point of the RPS. No measurable deformation was seen. This accurately represents the deformation of 0.0123 inches for a 300 pound side load and verifies that all the FEA for the RPS was accurately and correctly calculated, thus ensuring the vehicle has been sturdily and safely designed.

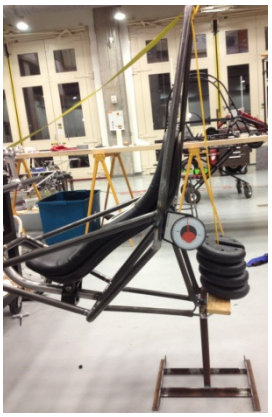

Figures 39 and 40: Vertical RPS Testing at a 12 Degree Angle

To test the structural integrity of the vehicle while under load of the rider the bike was firmly mounted in the riding position. With the seat in place a rider mounted the bike and the deformation of the spine was measured to be $1/16^{th}$ of an inch. This variable is slightly higher than expected but it likely due to compress in the rubber tire and not totally deformation of the spine itself. With all variables considered we are very pleased with the results and are comfortable in our conclusion that the bike is of a strong and supportive design.

b. Developmental Testing

Fairing Testing:

Testing was an important aspect in the design and optimization of the fairing. Since our group planned on fabricating the fairing out of carbon fiber, it was imperative to test various carbon fiber panels and layups to ensure strength and durability.

Initially, we laid up six layers (6 ply) of 3K plain weave carbon fiber, vacuum bagged the panel, and infused it with resin using standard VARTM processes. We then allowed twenty four hours at room temperature for the panel to cure. After the curing process, we cut the larger panel into three smaller panels and took multiple readings of dimensions to allow for the most certainty in our ASTM standardized tests [1]. We used these particular panels to perform a three-point

flexure test, using university equipment, to determine the bending capabilities and yield strength of the carbon fiber. Table 7 shows the results of the flexure testing.

Table 7: 3-point carbon fiber flexure test results

Measurement (mm.)	Sample	1 (mm)	2 (mm)	3 (mm)	4 (mm)	5 (mm)	AVERAGE (mm)
Thickness	SAMPLE 1	1.23	1.18	1.21	1.18	1.16	1.19
	SAMPLE 2	1.2	1.2	1.23	1.24	1.22	1.22
	SAMPLE 3	1.26	1.25	1.22	1.24	1.23	1.24
Width	SAMPLE 1	12.96	12.9	12.69	12.6	12.57	12.74
	SAMPLE 2	13.28	13.19	13.12	12.98	12.86	13.09
	SAMPLE 3	13.25	13.33	13.39	13.35	13.45	13.35

Sample	Flexural Strength (MPa)	Maximum Bending Moment	Moment of Inertia	Distance to Center (mm)	Yield Stress (psi)	Maximum Load (lbs.)
SAMPLE 1	705.060	2127.810	1.799	0.596	102260.248	50.353
SAMPLE 2	850.563	2751.960	1.970	0.609	123363.756	65.123
SAMPLE 3	856.869	2932.365	2.122	0.620	124278.371	69.392
AVERAGE	804.164	2604.045	1.964	0.608	116634.125	61.622

In order to calculate the stress experienced by the plate of carbon fiber, we used the beam theory equation for a rectangle cross-section that is fixed on each end with a load being applied at the center of the beam. This equation is given by

$$\sigma = \frac{Mc}{I} = \frac{3FL}{2bd^2} \tag{3}$$

where M is the maximum bending moment, c is the distance from the center of the specimen to the outer surface, I is the cross-sectional moment of inertia, F is the applied load, L is the specimen length, b is the specimen width, and d is the specimen thickness [1]. The results of this experiment allowed us to begin making decisions on the number of composite plies we thought would be suitable for our fairing. As seen above in Table 7, the 6 ply carbon fiber was incredibly resilient to loading and produced an average yield stress and maximum load on each small panel of $117\ ksi$ and $62\ lb$ respectively. In order to save as much weight as possible on the fairing, we determined that the use of 6 plies would not be required, especially considering our plan to incorporate honeycomb ribs. In addition, we also determined that using vacuum assisted resin transfer molding would not be practical for such a large and convex mold. Instead, we decided to utilize the standard wet layup and vacuum bag approach to minimize excess resin without too much difficulty.

In addition to the flexure test, we conducted an abrasion test to get an idea of what could happen to our fairing if we were to wreck and slide across the ground. To perform this test we tacky taped a 37 lb. aluminum block to the top of each 7.5 in. x 7.5 in. panel separately, secured the block to the back of a bicycle, accelerated the block with the bike to 10 mph, and traveled a distance of 30 ft. across concrete at constant velocity. Utilizing this method creates a constant pressure of 0.658 psi on the composite plate, which we believe is an accurate force considering

the contact area and weight of our vehicle during a crash. Unfortunately, 10 mph is not our maximum speed, but this speed does serve to show the characteristics of each composite plate for comparison.

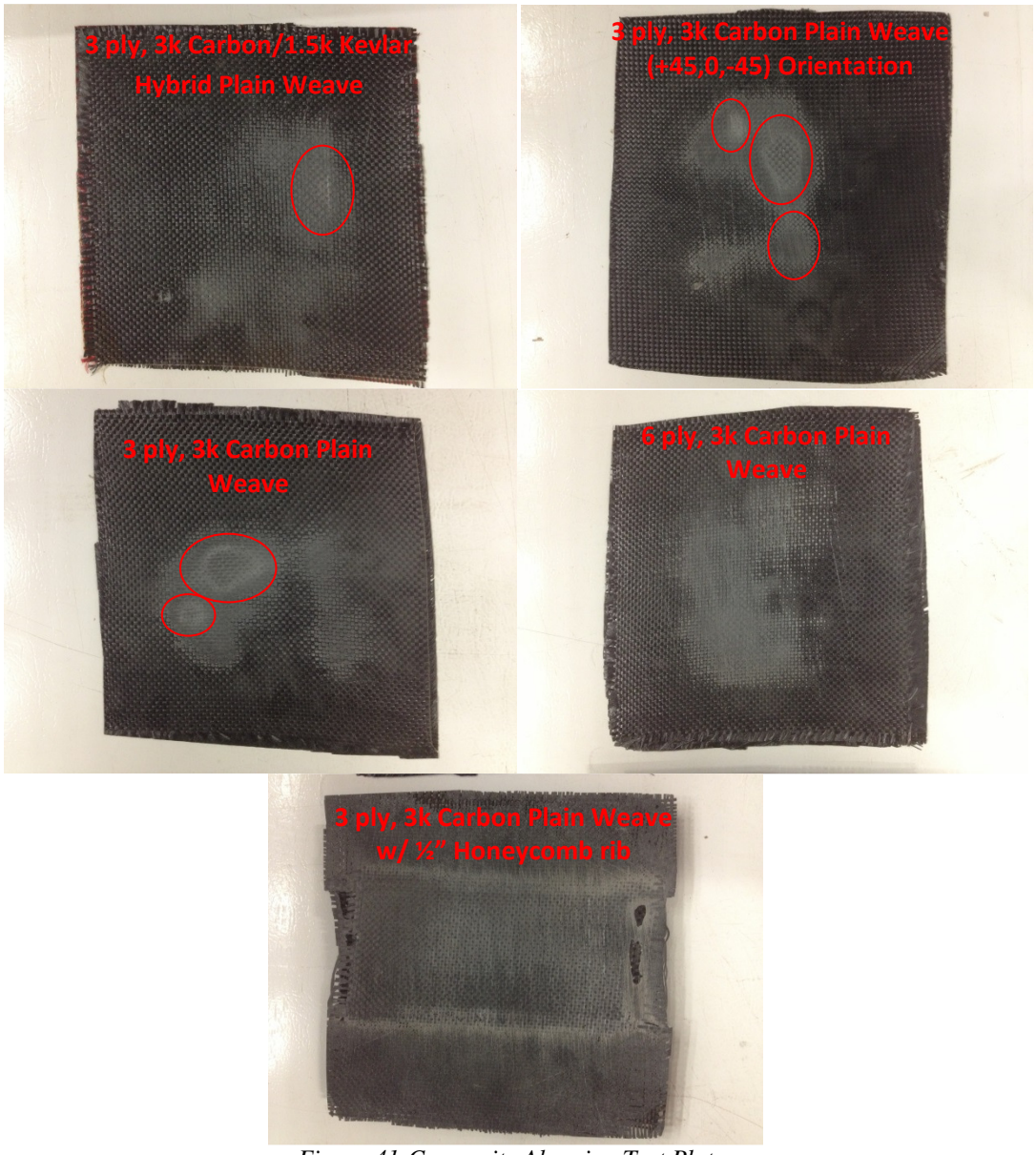

Figure 41:Composite Abrasion Test Plates

Table 8: Abrasion Test Results

Abrasion Test Results		
Specimen	**Weight (lb) (g)**	**Penetration (layers, locations)**
3 ply, 3k Carbon Fiber/1.5k Kevlar Hybrid Plain Weave	0.083 (37.5)	1 ,1
3 ply, 3k Carbon Fiber Plain Weave (+45,0,-45)	0.082 (37.1)	1,3
3 ply, 3k Carbon Fiber Plain Weave (90,0,90)	0.081 (36.8)	1,2
6 ply, 3k Carbon Fiber Plain Weave	0.167 (75.7)	0,0
3 ply, 3k Carbon Plain Weave w/ 1/2" Honeycomb Rib	0.118 (53.4)	0,0

The final test that was performed for the fairing analyses was to see whether or not honeycomb was worth adding to our fairing. To investigate this, we routed out a nosecone using MDF and laid up two different curved panels, one with honeycomb and one without. During this test, we used a wet layup technique and vacuum bagged them using a room temperature resin. The two nosecones are shown below.

Figure 42: Nose-Cone Composite Prototype

Once both of these panels had cured, they were inspected to compare the stiffness and the weight of each. While the panel with the honeycomb weighed approximately 25% more than panel without honeycomb (106.8 g and 142.7 g respectively), the stiffness was noticeably increased across the entire structure. Because the tip of the nosecone is such a complex curvature, the composite system is fairly rigid and strong at that point, but as force is exerted along the less concave edges the nosecone becomes much more flimsy.

c. Performance Testing

Landing Gear Suspension System:

The Crimson Edge's landing gear suspension system is an entirely new innovative concept from last year's vehicle, the Crimson Fury. Unlike the Crimson Fury, the Crimson Edge is a two wheeled recumbent bike and requires a greater amount of stability to ride the vehicle at slower speeds. In order to do so, the design team added a landing gear system much like the landing gear of an airplane or the training wheels of a children's bike. However, contrary to other schools vehicle landing gear designs, the Crimson Edge has a spring suspension system rather than just straight rigid rods. This allows the landing gear to absorb any irregular forces due to uneven terrain and still maximize the vehicles stability.

To determine whether or not the suspension system would function as predicted the landing gear was subjected to cyclic compression loading of 200 lbs., which is 60 lbs. more than half the overall weight of the vehicle and the team's heaviest rider. After loading and unloading the landing gear suspension system nearly 300 times, the suspension spring system still functioned as designed and the custom fabricated springs with variable spring constants were still fully functional. The design team did learn, however, that applying lubrication periodically to the concentric pipes increased the overall smoothness of the compression loading, which would allow for a much smoother ride for the vehicle rider during competition. Therefore, the design team will be thoroughly lubricating the concentric pipes of the landing gear system multiple times throughout the competition to decrease the fatigue of the suspension system and to maximize the smoothness of the vehicle. Images taken during the cyclic compression loading can be seen below.

Figure 43: Landing Gear Cyclic Loading Testing

Safety

Safety was one of the primary concerns when designing the vehicle. Throughout the design phase, each component of the vehicle was thoroughly analyzed to meet the requirements set by the HPVC and a minimum safety factor of 2 was required by all components. If a component did not meet these requirements, however, it was redesigned until all constraints were met. Specific components of the bike were designed with a direct goal of maximizing safety for the rider. In addition to the rollover protection system (RPS), the landing gear stabilization system of the vehicle provides increased stability for the vehicle at slow speeds and during sharp turns and the full carbon fiber fairing with Nomex honeycomb ribs for reinforcement provides a sturdy, protective shell for the rider in the event that the vehicle were to wreck or fall over.

During the fabrication phase, safety was maintained as a top priority. All design team members were required to wear safety glasses and to abide by all machine shop rules set by our University machine shop director. Additionally, each member of our team went through a safety workshop provided directly by our machine shop director prior to working in the shop or using machinery. Further safety precautions that were taken during manufacturing included protecting the welders by requiring that proper clothing and leather protection be worn by all welders. Team members were also required to be accompanied by at least one other team member when working in the

shop. Lastly, any sharp edges that were initially designed were either chamfered or lined in order to prevent any harm of other fabricator's and potential riders.
In order to remain safe while fabricating the various testing layups and preparing the fairing mold, proper safety equipment and facilities were utilized. When performing wet layups and using the epoxy resin system, latex gloves and brushes were used to handle and spread the resin after mixing. In addition, gloves, eye protection, and air filter face masks were used in a well-ventilated area when sanding the 2-lb polyurethane foam, using the gap & crack foam, and applying bondo in order to protect team members.
For the competition, not only is the rider's safety a major concern, but their health as well. Each rider must be fully aware of the physical demands that are required by the competition and of their own physical limitations. If the rider feels short winded or faint, that rider will be required to stop and a replacement rider will take his or her place. In hopes of preventing this in the first place, the members of our team have been physically training throughout the semester to ensure they are in good physical shape to competitively race in the ASME HPVC competition. Additionally, riders are required to wear a safety helmet that meets all the HPVC requirements set by ASME. The vehicle also has a full shoulder seatbelt that must be worn at all times. If a rider fails to meet any of these requirements, he or she will not be allowed to compete.

Aesthetics

Aesthetics were addressed in a number of ways during the design of our bicycle. One way by which we addressed aesthetics was the use of a full fairing. Having seen teams at previous competition teams with full fairings, we realized how sleek and professional their bikes looked compared with others with partial fairings. Since we are using a full fairing, we will be able to paint the entirety of the outside portion of our bicycle, giving a clean outward appearance. Another aesthetical decision is the implementation of the retractable landing gear with a suspension system. While some teams we saw at competition last year did use a retractable landing gear, we did not see any that included suspension. We believe this addition will make our bike stand out and be visually appealing.

Conclusions

a. Evaluation

The final vehicle matches very well with the design objectives that our team established. We sought to have a vehicle that was safe, stable, durable and comfortable for the rider. We are certain that our bicycle is safe because of all of the FEA that we have simulated, as well as the physical tests that we have performed; our bike should not fail under normal operating conditions. Our vehicle promises to be fast, based on projections that we have made during the design process. The fairing contributes considerable reduction in drag, and the drivetrain is designed to produce high speeds. Lastly, our bike should be comfortable. The bike is sized in a way that is comfortable for a conventional rider. The adjustable pedaling system and the adjustable handlebar position allows for a rider to have a more customized ride. All aspects of the bicycle should produce a bicycle that will be comfortable and easy to be ridden.

b. Recommendations

There are some modifications and improvements that could be made in the future for our vehicle. A potential modification of our vehicle would be to bend the handlebars in an ideal shape to both give the rider comfort while avoiding the rider's knees while pedaling. One such improvement

would be the use of frame piping with a smaller wall thickness. Given our factors of safety for the entirety of the frame was considerably higher than 2, using smaller wall thickness would greatly reduce the overall weight of the vehicle. Another such improvement would be a slimmer width for our frame. Having a smaller width would greatly reduce the size of our vehicle, which would ultimately make it more aerodynamic.

c. Conclusion

Overall, our vehicle's design was completed in accordance with all of our design objectives: safety, speed, and comfort for riders of a variety of sizes and abilities. As discussed earlier in this report, safety was our main objective. Throughout the design process, we were consistently finding safety factors that were considerably higher than needed, thus ensuring our vehicle's safety in the event of a catastrophic event during the competition. Additionally, the fairing that was designed also adds substantial value to our vehicle's overall safety.

Speed, another major concern, was addressed in a number of ways. The use of the fairing greatly reduced the drag for the speed portion of competition. As seen in the aerodynamic analysis section, at higher speeds the fairing became more effective at reducing drag, making the vehicle perform at a high level.

Finally, comfort was thoroughly included in the design of the bike. The padded seat that was used in our bike was just one aspect of the design that added to the comfort. Another aspect includes the roll cage extending a few inches past our shoulders, giving the rider a more relaxed position while riding.

In conclusion, our recumbent bicycle met all of our initial design requirements, as well as competition standards. Since this is our team's first recent design of a two-wheeled bicycle, we think we will be more competitive this year and it will be a great steppingstone for the Sooner Powered Vehicle team in the future.

References

Fairing References:

[1] ASTM Draft Standard, "Standard Test Methods for Flexural Properties of Fiber-Reinforced Polymer Matrix Composites," ASTM International, W. Conshohocken, Pa. (in preparation).

[2] Battles, Christopher. "QFD: House of Quality Template." QFD: House of Quality Template. N.p., 23 Apr. 2010. Web. 15 Sept. 2012. <http://www.schrodingersghost.com/?p=399>.

[3] "Composite Materials." *Aircraftspruce.com*. Aircraft Spruce, n.d. Web. 1 Feb. 2013. <http://www.aircraftspruce.com/pdf/2013Individual/Cat13CM.pdf>.

[4] Dellinger, Dan. "Wind- Average Wind Speed- (MPH)." *National Climatic Data Center*. 20 Aug. 2008. Web. 1 Mar. 2011. <http://lwf.ncdc.noaa.gov/oa/climate/online/ccd/avgwind.html>.

[5] Faulkner, L. L., ed. *American Chain Association Standard Handbook of Chains: Chains for Power Transmission and Material Handlind, Second Edition*. Boca Raton, FL: CRC Press, 2006. Print.

[6] Global, "Mill/Drill Head PF 230," <http://www.globalindustrial.com>, accessed March 4, 2013

[7] Hoffmann, "Morso NFL Manual Notching Machine," <http://hoffmann-usa.com/morso-nfl-manual-notching-machine>, accessed March 4, 2013.

[8] Home Depot, "Pro-Series 120-Volt Arc Welder," <http://www.homedepot.com>, accessed March 4, 2013.

[9] Juvinall, Robert C., and Kurt M. Marshek. *Fundamentals of Machine Component Design*. New York: J. Wiley, 1991. Print.

[10] Lexington Bike Shop, Lexington, OK. <http://www.bicycle-stuff.com/main/bent/okrrb/index.html>

[?] Eley, Daniel, "The Physics of Bicycles," The University of Oklahoma, Spring 2013.

[11] Morgan, J.E., and Wagg, D.J., 2002,"The Failure of Bike Cranks, International Standards, Tests and Interpretations",Sports Engineering,pp. 113-119

[12] Northern Tool, "Klutch Sander Polisher," Northern Tool Website, <http://www.northerntool.com>, accessed March 4, 2013.

[13] RayPlex Composite Technology, "The Fundamentals of Fiberglass." *Fundamentals of Fiberglass.* Web. 25 Feb. 2013. <http://www.fibreglass.com/HOWTO/k-fun-fibre.htm>

[14] Summit Racing, "Woodward Fab Nanual Tube and Pipe Benders WFB2," <http://www.summitracing.com/parts>, accessed March 4, 2013.

[15] "Woven Fabrics." *Net Composites*. EcoComp, n.d. Web. 1 Feb. 2013. <http://www.netcomposites.com/guide/woven-fabrics/40>.

[16] Harry, Ryan. "Rake, Head Tube Angle, and Trail." *HarryRyan.com.* Web. 12 Feb. 2013. <http://ryanharry.com/archives/843>.

Appendix I: Project Schedule

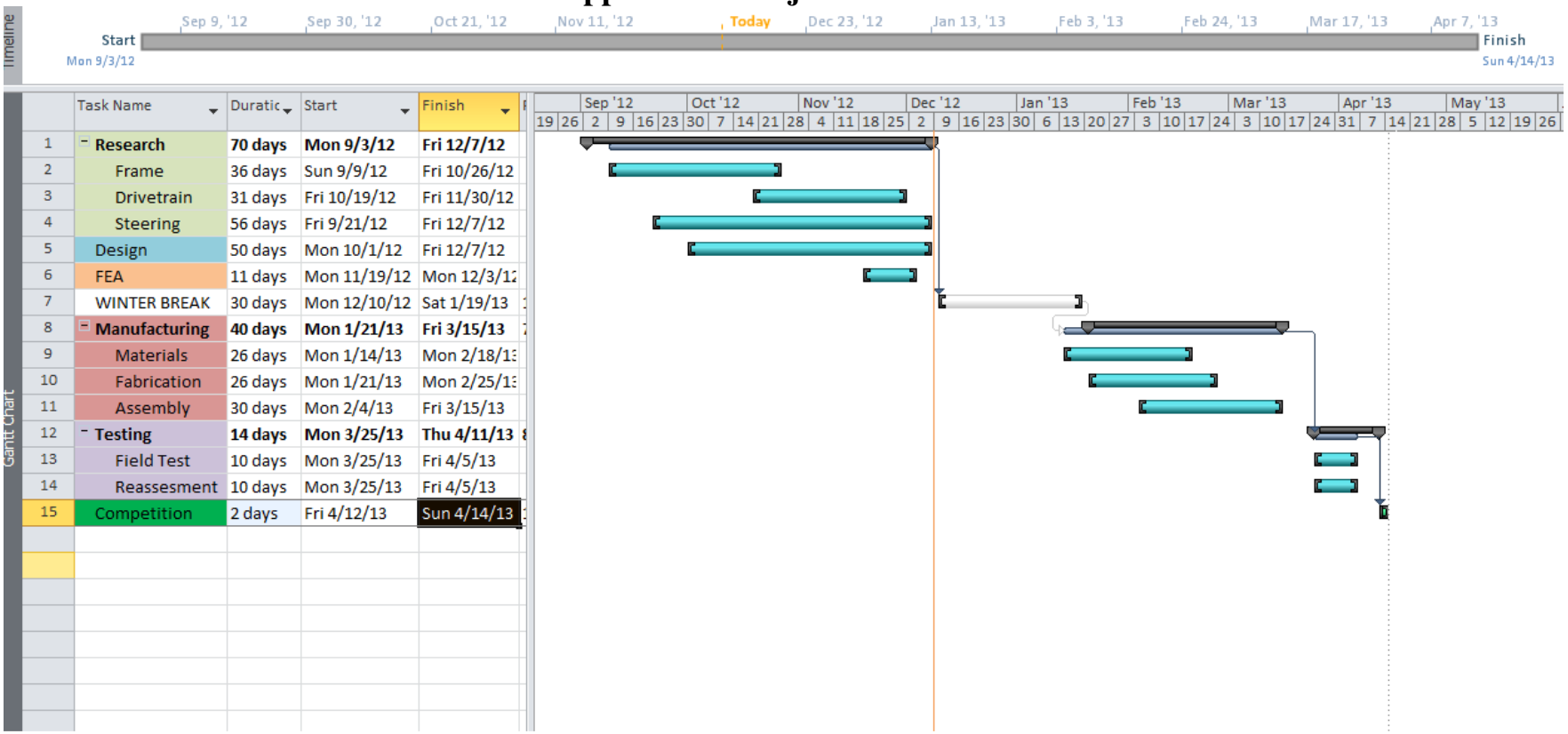

The Gantt chart project timeline for the 2012-2013 Sooner Powered Vehicle was created in Microsoft Project, and it incorporated timeline goals in the areas of Research, Design, FEA (and other analysis), Manufacturing, and Testing.